Research Article

Characterization of NACA 2412 and NACA 4412 airfoils: Effects of angle of attack on aerodynamics coefficients

Dilsad AKGUMUS GOK[1],* , Khaled Nimer Mohammad AL-NIMER[1]

[1]Department of Mechanical Engineering, Istanbul Aydin University, Istanbul, 34295, Türkiye

ARTICLE INFO

ABSTRACT

The angle of attack plays a pivotal role in determining the performance of an aircraft wing, a critical component of its overall design. This angle, defined as the angle between the chord line of the wing and the relative wind direction, has a profound impact on the lift and drag forces experienced by the wing. When the angle of attack is low, the wing generates lift with minimal drag. However, at higher angles of attack, the wing encounters increased drag and may reach a stall condition.

Understanding the influence of the angle of attack on an aircraft wing is crucial in both design and operation, significantly impacting the aircraft's capabilities in takeoff, climb, navigation, and landing. Therefore, a comprehensive comprehension of the relationship between the angle of attack and wing performance is imperative for ensuring safe and efficient aircraft operation. This study is dedicated to elucidating the effect of the angle of attack on aircraft performance, focusing on the variation in aerodynamic coefficients for two distinct airfoils. Employing Computational Fluid Dynamics (CFD) analysis via SolidWorks, the research examines NACA airfoil types, specifically NACA 2412 and NACA 4412, each featuring different cambers. The selected angles of attack for the investigation range from 0° to 20°, with a constant flow rate of 43 m/s. The findings reveal that the NACA 2412 airfoil exhibits a higher lift-to-drag ratio near to 20 compared to 6 in NACA 4412 airfoil. This insight provides valuable information for optimizing the aerodynamic performance of aircraft wings, contributing to the enhancement of overall efficiency and safety in aviation.

Cite this article as: Akgumus Gok D, Al-Nimer KNM Characterization of NACA 2412 and NACA 4412 airfoils: Effects of angle of attack on aerodynamics coefficients. J Ther Eng 2024;10(6):1524–1538.

INTRODUCTION

In recent years, Computational Fluid Dynamics (CFD) analysis has become an essential tool for studying the aerodynamic performance of airfoils [1]. Airfoils play a crucial role in various engineering applications, including aircraft wings, wind turbine blades, and other aerodynamic structures. Understanding the behavior of airfoils and their response to different operating conditions is vital for

optimizing their performance and improving overall efficiency [1].

Several studies have been conducted to investigate the aerodynamics of different airfoil shapes and their performance under various flow conditions [1]. The NACA 2412 airfoil, in particular, has been the subject of numerous investigations in recent years. For instance, a study comparing the power, lift, and drag coefficients of wind turbine blades using the aerodynamic characteristics of the NACA0012 and NACA 2412 airfoils reported significant differences in their performance [1]. Similarly, FEM/CFD analysis of wings at different angles of attack provided insights into the behavior of the NACA 2412 airfoil under varying flow conditions [2].

The COMSOL Multiphysics Simulation program was employed to conduct a comprehensive analysis of drag coefficients (CD), lift coefficients (CL), and the glide ratio (CL/CD) for five different airfoils—specifically, NACA 2412, NACA 2415, NACA 2418, NACA 4412, and NACA 4415. The simulations were carried out for two Reynolds numbers, 1×10^5 and 2×10^5, capturing a range of flow conditions. The angle of attack (α) was systematically varied from 0° to 10° to investigate its impact on the aerodynamic performance of the airfoils [3]. The imperative for more efficient design has become a primary focus, particularly in addressing a broad range of angles of attack (AOA) to mitigate stall formation. This project involves a comparative analysis between two categories of NACA series airfoils: symmetrical and asymmetrical profiles, each tailored for specific applications across various sectors. The airfoil profiles are integrated into ANSYS Fluent through data files, facilitating a 2D simulation of the airfoils under two distinct wind velocities, namely 3 m/s and 15 m/s [4].

The modeling and numerical analysis were executed using commercially available Computational Fluid Dynamics (CFD) software. This approach is preferred due to its cost-effectiveness compared to experimental methods. Computational methods are increasingly favored, and the numerical results obtained in this study align well with theoretical expectations. This alignment reinforces the reliability of Computational Fluid Dynamics (CFD) as a credible and practical alternative to experimental procedures, particularly when assessing the aerodynamic performance of airfoils [5]. The primary objectives was to conduct a comparative analysis of four airfoils—NACA 2412, NACA 4412, NACA 23012, and NACA 23112—at various angles of attack while maintaining a constant Reynolds number. The geometric modeling and analysis were performed using Ansys-Fluent, and the Computational Fluid Dynamics (CFD) study employed the SST K-w model. The calculations encompassed a range of attack angles [6].

Moreover, investigations into the aerodynamic analysis of aircraft wings have highlighted the importance of understanding the underlying principles governing the airflow around airfoils [7]. Additionally, CFD simulations have been employed to explore the effects of modified cavity shapes on the aerodynamic performance of the NACA 2412 airfoil [8]. Furthermore, the aerodynamic performance of the NACA 2412 airfoil at low Reynolds numbers has been investigated, shedding light on its behavior in low-speed applications [9]. The design optimization and analysis of the NACA 0012 airfoil using computational fluid dynamics and genetic algorithms have also been carried out, demonstrating the potential for improving airfoil performance through advanced optimization techniques [10]. Studies have shown that the performance of airfoils is influenced by factors such as the Reynolds number, angle of attack (AOA), and other geometric modifications [11]. The effect of the Reynolds number on the performance of a modified NACA 2412 airfoil has been explored, highlighting the need for considering flow conditions in the analysis [11]. Additionally, aerodynamic performance comparisons have been made for airfoils suggested for small horizontal axis wind turbines, emphasizing the importance of selecting suitable airfoil profiles for efficient energy conversion [12]. Considering the significance of low Reynolds number airfoils in small horizontal axis wind turbines, the design of an optimized airfoil for such applications has also been investigated [13]. In the field of turbulence modeling, research has been focused on developing advanced techniques to accurately predict turbulent flows, contributing to a more precise analysis of airfoil aerodynamics [14]. The aerodynamic performance of a bladeless fan, the effects of outlet thickness and outlet angle were examined using numerical methods. In the analyzes performed on five different airfoil profiles (Eppler 479, Eppler 169, Eppler 473, S1046 and S1048), a network model was created with the volume finite element method using ANSYS ICEM CFD 16.0 and ANSYS CFX 16.0 and boundary conditions were applied. In the study, the outlet thickness varied between 0.8 mm and 2 mm, the outlet angle varied between 20° and 80°, while the inlet volumetric flow rate was adjusted from 5 LPS to 80 LPS. It was found that the Eppler 473 airfoil exhibited the best performance with a constant exit thickness of 1 mm and exit angle of 70°. The results revealed that the exit thickness has a more significant effect than the exit angle in determining aerodynamic performance [15]. The effects of camber ratio on flow characteristics on different airfoils were examined experimentally and numerically. In the experiments and simulations performed on NACA 4412, NACA 4415 and NACA 2415 profiles, the Reynolds number was determined as 1×10^5 and the angle of attack was 8°. The formation of laminar separation bubble and boundary layer separation was observed with experimental data. It has been determined that as the camber ratio increases in the NACA 4412 airfoil, the laminar separation bubble shortens and the transition point shifts forward. The results show that the camber ratio and thickness variation significantly affect the boundary layer separation and bubble development [16]. The effect of the slotted flap on the aerodynamic performance of the NACA 24012 airfoil was examined numerically. In the study, the effects of flap chord

ratio, clearance and overlap on the wing were tested at zero angle of attack with slotted flap models with 20%, 30% and 40% chord ratios. Flap distance was adjusted using dynamic network and user-defined functions and 2D Fluent analyzes were performed under conditions with Reynolds number of 3.1×10^6. The results showed that larger flap beam ratio increased the lift coefficient but additionally resulted in a drag penalty. Additionally, the lift loss achieved with 3% C flap extension was found to be significant. It has been stated that the highest lift coefficient is achieved with 1% C space. [17]. The aerodynamic performance of wings with NACA0012 cross-section and the effects of sinusoidal entry edge and exit edge were examined. It is aimed to increase wing performance by using sinusoidal fold, delay fatigue phenomenon at high angles of attack and improve aerodynamic performance. Using the ANSYS FLUENT method, the aerodynamic performance of wings with different sinusoidal edges and a simple wing at Reynolds numbers of 5000, 15000 and 60000 was simulated numerically. In the study, governing equations were solved with the transition SST-4EQ method. The results showed that the maximum pressure around the wing with a sinusoidal edge was higher than that of the simple wing. However, it has been observed that the drag value of this geometry is the highest compared to other wing types. [18].

Furthermore, investigations into the effects of dimples and virtual gurney flaps on airfoil performance have demonstrated the potential for flow control and enhancement of aerodynamic efficiency [19, 20].

The present study focuses on the NACA 2412 and NACA 4412 airfoils, which have been extensively studied due to their widespread usage and well documented aerodynamic characteristics. In addition, the objective of this study is to conduct a comprehensive analysis of the aerodynamic performance of two distinct airfoils, namely NACA 2412 and NACA 4412. This analysis is carried out through the utilization of Computational Fluid Dynamics (CFD) simulations. The aim is to delve into the intricate aerodynamic characteristics of these airfoils, providing valuable insights into their performance under varying conditions. By employing advanced simulation techniques, the study seeks to enhance our understanding of the flow patterns, lift, drag, and other critical aerodynamic parameters associated with the NACA 2412 and NACA 4412 airfoils. Such insights contribute to the broader field of aerodynamics and can have practical implications for optimizing the design and performance of aircraft wings.

THEORY AND METHOD

When an airfoil is subjected to a high angle of attack, the flow separation can occur, leading to a phenomenon called "stall." Stall is characterized by a sudden drop in lift and an increase in drag, which can significantly reduce the aerodynamic efficiency of the airfoil. The exact mechanism of stall is complex and depends on various factors such as the shape of the airfoil, the Reynolds number, and the turbulence of the flow. To mitigate the effects of stall, engineers have developed various techniques such as using stall strips, vortex generators, and active flow control methods. Understanding the phenomenon of stall is crucial for designing efficient aerodynamic structures, such as airplane wings, wind turbine blades, and racing car spoilers [21]. Figure 1 shows that the effect of angle of attack against the wind flow.

The angle of attack was changed from 0° to the stall angle to get a complete picture of the behavior of the airfoil. In order to obtain accurate results, the K-epsilon RNG turbulence model was chosen and the governing equations were solved using quadratic methods. The simulations conducted in this study were executed within a steady-state environment. This choice enables the capture of the airfoil's stable behavior under diverse conditions. By adopting a steady-state approach, the study aims to analyze and understand the consistent and unchanging flow patterns around the NACA 2412 and NACA 4412 airfoils. This methodological decision facilitates a focused examination of the airfoils' aerodynamic performance, providing insights into their stability and behavior across various scenarios. The use of

Table 1. Applied conditions

Position	Condition
Edge	Condition applied
Inlet	Velocity
Outlet	Pressure
Top Wall	No slip
Bottom Wall	No slip
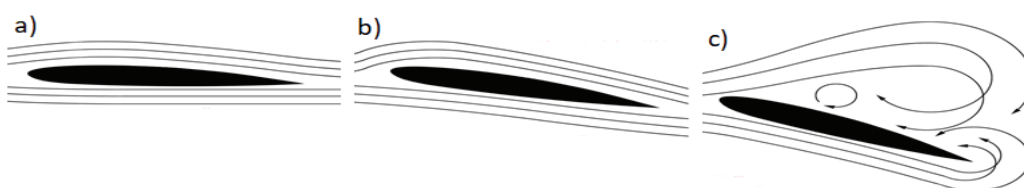
Figure 1. a) Low, b) High, c) Stalling angle of attack.

steady-state simulations allows for a detailed exploration of the airfoils' characteristics under different conditions as shown in Table 1, contributing to a comprehensive understanding of their aerodynamic responses.

The governing equations for fluid dynamics are the Navier-Stokes equations, which describe the motion of fluid particles subject to external forces. The equations are written in terms of the velocity vector, v, the pressure, p, the density, ρ, and the viscosity, μ, and are given by:

Conservation of mass:

$$\frac{\partial \rho}{\partial t} + \nabla \cdot (\rho v) = 0 \tag{1}$$

Conservation of momentum:

$$\rho[\partial v / \partial t + (v \cdot \nabla)v] = -\nabla p + \mu \nabla^2 v + f \tag{2}$$

where f represents any external forces acting on the fluid. These equations describe the motion of a fluid under the influence of external forces, such as the forces exerted on an airfoil by the surrounding air. When simulating the fluid dynamics around a rotating blade, a frame of reference rotating with the blade can be used, in which case the equations are modified to:

Conservation of momentum:

$$\rho \left[\frac{\partial vr}{\partial t} + (vr \cdot \nabla)vr + 2\omega \times vr\right] = -\nabla p + \mu \nabla^{2vr} + f \tag{3}$$

where vr is the relative velocity (the velocity viewed from the rotating frame) and ω is the angular velocity. These equations can be solved numerically using CFD.

The K-epsilon model is widely used for turbulence modeling, although its performance is limited in cases of large adverse pressure gradients . This two-equation model includes two extra transport equations that represent the turbulent properties of the flow, allowing for the modeling of history effects such as convection and diffusion of turbulent energy. The first transported variable, k, represents turbulent kinetic energy, while the second transported variable, ε, represents turbulent dissipation and determines the scale of turbulence. In contrast, k determines the energy in turbulence. The RNG model is a variation of the K-epsilon model that utilizes Re-Normalization Group (RNG) methods to renormalize the Navier-Stokes equations, accounting for the effects of smaller scales of motion [10]. The two airfoils, to which the analysis will be applied, are presented in Figure 2 and Table 2.

The utilization of FLUENT is pivotal in conducting Computational Fluid Dynamics (CFD) analysis, as it establishes the working environment for simulating objects. A critical step involves creating a mesh that spans the entire object, extending in all directions to incorporate the physical properties of the surrounding fluid (air). To apply necessary boundary conditions for analysis, it is essential to group the mesh and edges effectively. The process begins by importing the coordinates of the airfoils and generating

Table 2. Airfoils dimentions [22]

Airfoil	Max thickness	Max camber	Chord length (mm)
NACA 2412	12% at 30% chord	2% at 40% chord	1000
NACA 4412	12% at 30% chord	4% at 40% chord	1000
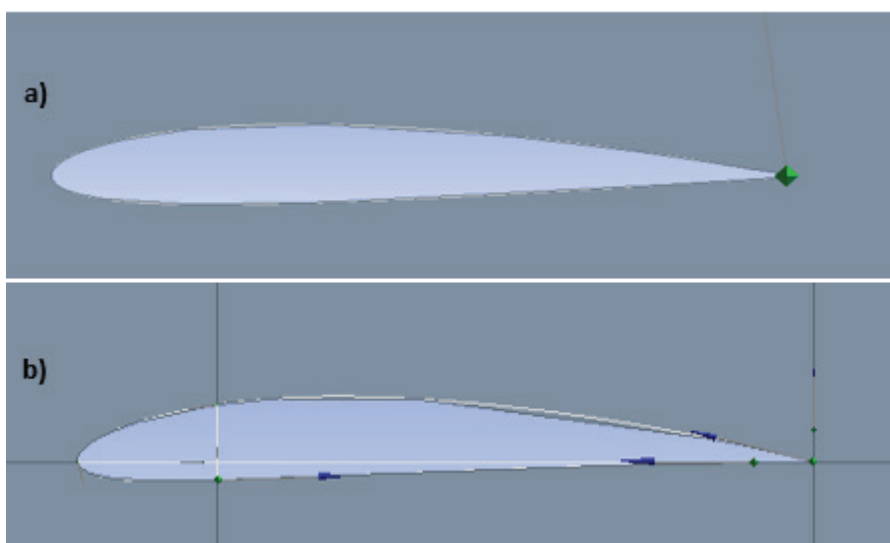
Figure 2. a) NACA 2412 airfoil, b) NACA 4412 airfoil cross sections.

a curve through 2D analysis, followed by launching the design model. Subsequently, the desired size of the domain for the airfoils section is drawn. The coordinate system can be established either at the trailing edge of the airfoil, facilitating the creation of a rectangular mesh domain geometry using dimension tools.

While a three-dimensional study can potentially yield more comprehensive results, it's noted that in this case, a 2D analysis has been deemed sufficient. Despite the simplicity of the two-dimensional approach, it is expected to provide satisfactory results for the specific scenario under consideration. The decision to opt for 2D analysis may be influenced by factors such as computational efficiency, resource constraints, or the nature of the problem, where the added complexity of a three-dimensional study may not significantly enhance the accuracy of the results.

The parameters of the test shown in Table 3 acts like boundery conditions of airfoils and the properties of flow around it.

Reynolds numbers ranging from 50,000 to 500,000 are commonly referred to as the low Reynolds number regime. In this range, the flow exhibits fundamental differences and increased complexity compared to high Reynolds numbers. The transition process in this regime is characterized by neither an abrupt shift nor a typical occurrence while the boundary layer is attached to the airfoil.

Table 3. Test parameters

Parameter	Value
Fluid	Air
Velocity	43 m/s
Density	1.225 kg/m³
Angle of attack	0°, 5°, 10°, 15°, 20°
Chord length	0.1 m
Momentum	2nd order up wind scheme
Turbulent viscosity	0.0001460735 m/s
Number of iterations	1000

When the velocity reaches 43 m/s, the corresponding Reynolds number is 605,335. This particular case warrants attention in the study due to its inherent complexity, The Realizable k–ε turbulence model was devised to address the limitations of the standard model. It achieves this by adhering to mathematical constraints on the Reynolds stresses, ensuring consistency with the underlying physics of turbulent flows.

A finer mesh necessitates a greater number of computations, leading to prolonged simulation times. In the case of NACA airfoils, the spacing between nodes progressively widens from the leading edge. An even distribution of points is analyzed from the airfoil's maximum thickness point to its trailing edge. The mesh domain depicted in Figure 3.

For steady-state calculations, it is recommended to keep the iterations within the range of 1000 to 2000 iterations. On the other hand, for unsteady calculations, the ANSYS manual suggests using 20 iterations per time step. However, it's worth noting that in some cases, it may be necessary to increase the number of iterations, such as to 30 or 40, particularly at the initial stages of the calculation. Adjusting the iteration count allows for a balance between computational accuracy and efficiency, ensuring convergence in both steady and unsteady simulations [23, 24].

RESULTS AND DISCUSSION

This section will be a comprehensive analysis and comparison of the outcomes from each experiment. This study focuses on the influence of altering the airfoil's angle of attack on lift and drag forces. Notably, as the angle of attack varies, the results also changes, like drag and lift coefficients (CL), as well as variations in pressure distribution.

The first part of results will be the contours of velocity and pressure around the airfoils, Figure 4 shows that the velocity and pressure distribution around NACA 2412 when angle of attack equals to zero.

When applying the same boundary condition to NACA 4412, the distribution of velocity and pressure changes as
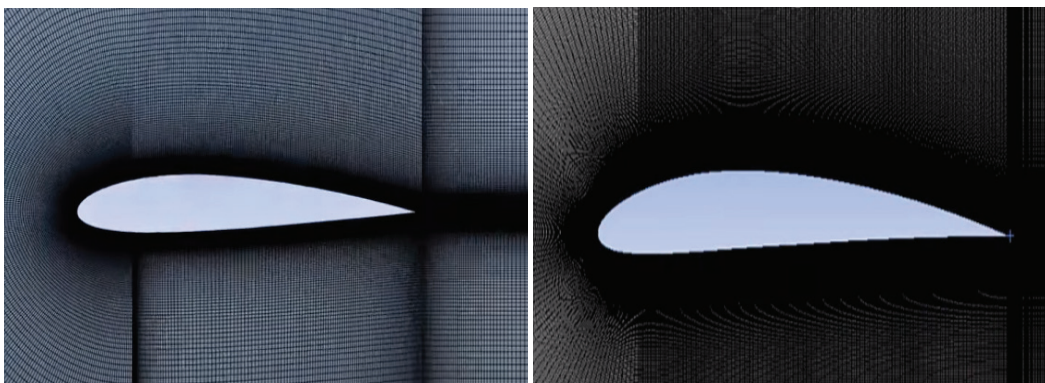
Figure 3. Mesh for NACA 2412 and NACA 4412.
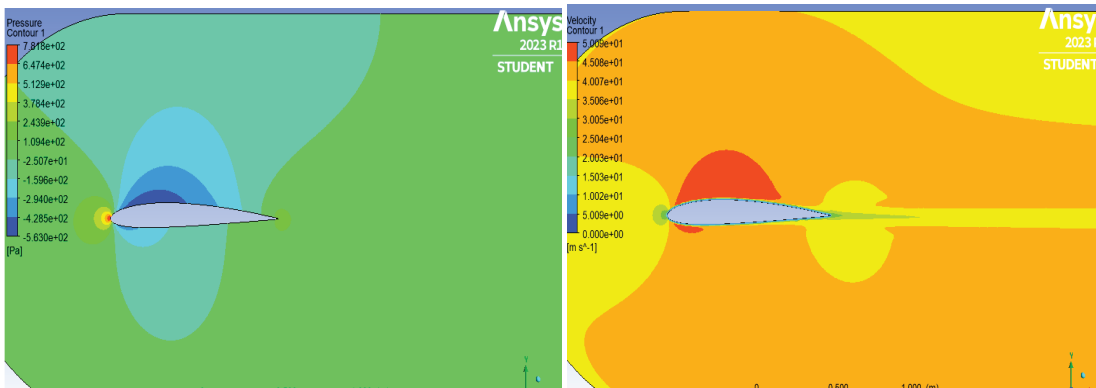
Figure 4. NACA 2412 airfoil pressure and velocity contour (Angle of attack = 0°).
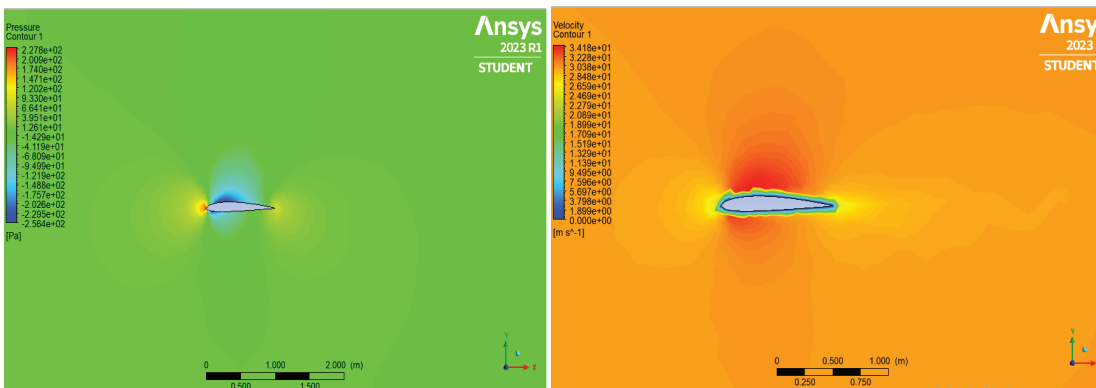
Figure 5. NACA 4412 airfoil pressure and velocity contour (Angle of attack = 0°).

Table 4. Angle of attack = 0°

AOA = 0°	Lift Force [N]	Drag Force [N]
NACA 2412	4.03	0.26
NACA 4412	88.61	14.43

it can be seen in Figure 5. And from this step of test the lift and drag forces was calculated and the values shown at Table 4.

When the angle of attack changes from zero to five the velocity and pressure contours was changed for NACA 2412 and NACA 4412 as shown in Figure 6 and Figure 7 respectively, it is clear from figures the difference in pressure that generate more lift force.

When the angle of attack increases to 5°, the change in lift and drag forces shown in Table 5 is observed.

The 3rd step of the test is changing the angle of attack to 10°. When examining this situation, Figure 8 and Figure 9 clearly show the velocity and pressure lines and the pressure difference between the lower and upper edges of the two airfoils.

In this particular case, a discernible trend emerges in the aerodynamic forces, as evident from the values of lift and drag forces presented in Table 6. Notably, there is a noticeable increase in these forces. Importantly, the lift-to-drag ratio is found to be more favorable in the case of the NACA 2412 airfoil compared to the NACA 4412 airfoil.

This observation underscores the superior efficiency of the NACA 2412 airfoil in terms of its lift-to-drag ratio, implying that it is more effective in generating lift relative to the drag experienced. Such findings provide valuable insights into the comparative aerodynamic performance of the two airfoils, contributing to a nuanced understanding of their respective capabilities and effectiveness in practical applications.

In this case, the increase in aerodynamic forces, the lift and drag force values shown in Table 6, shows that the lift/drag ratio is more effective in NACA 2412 than in NACA 4412.

Figure 10 and Figure 11 presents the starting of stall and separation of air flow from the airfoils and this phenomenon cause the decrease in lift force in two airfoils, in another word part from the flow was lost without generate any lift force.
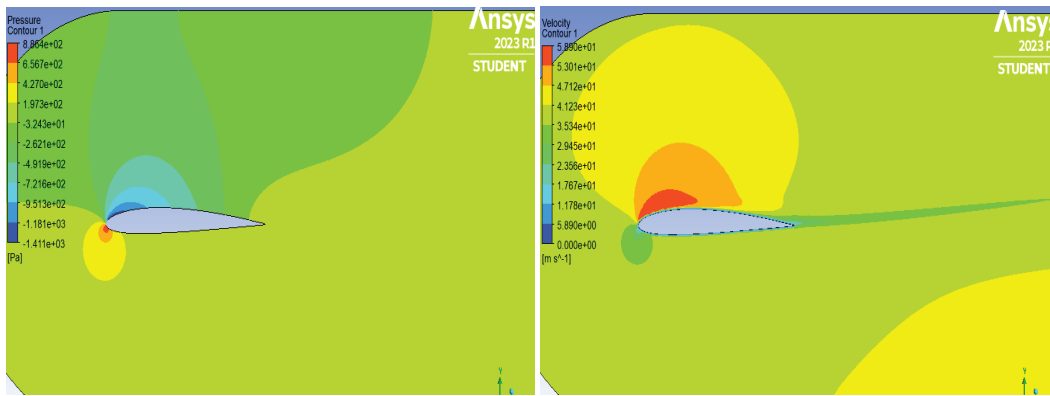
Figure 6. NACA 2412 airfoil pressure and velocity contour (Angle of attack = 5°).
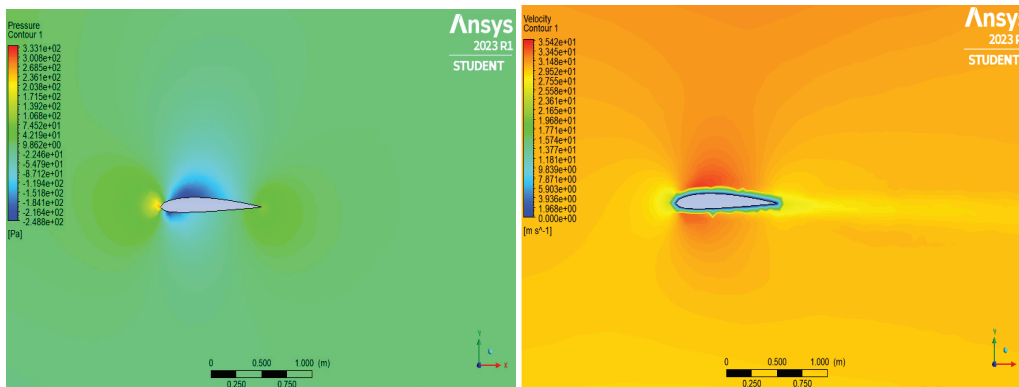
Figure 7. NACA 4412 airfoil pressure and velocity contour (Angle of attack = 5°).

Table 5. Angle of attack = 5°

AOA = 5°	Lift Force [N]	Drag Force [N]
NACA 2412	14.30	0.75
NACA 4412	89.95	14.94

Table 6. Angle of attack = 10°

AOA = 10°	Lift Force [N]	Drag Force [N]
NACA 2412	20.69	2.22
NACA 4412	92.81	15.44
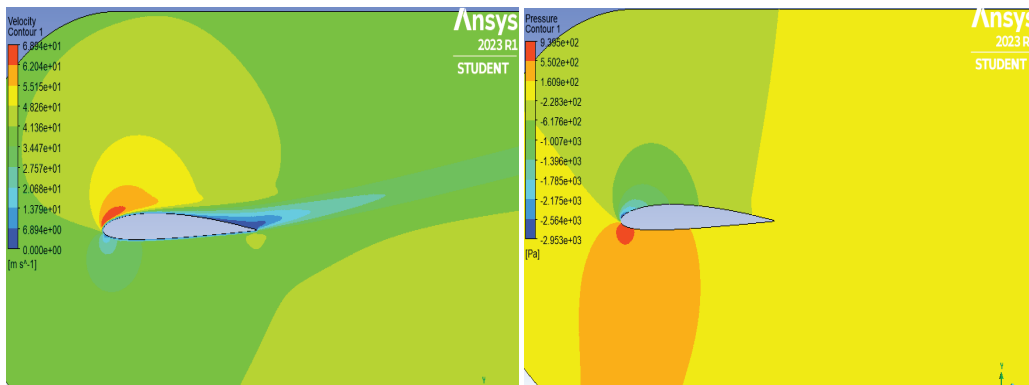
Figure 8. NACA 2412 airfoil pressure and velocity contour (Angle of attack = 10°).
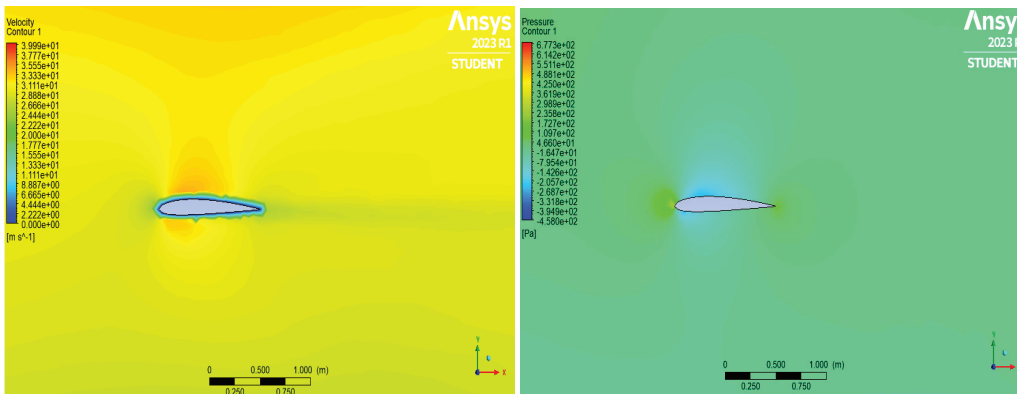
Figure 9. NACA 4412 airfoil pressure and velocity contour (Angle of attack = 10°).
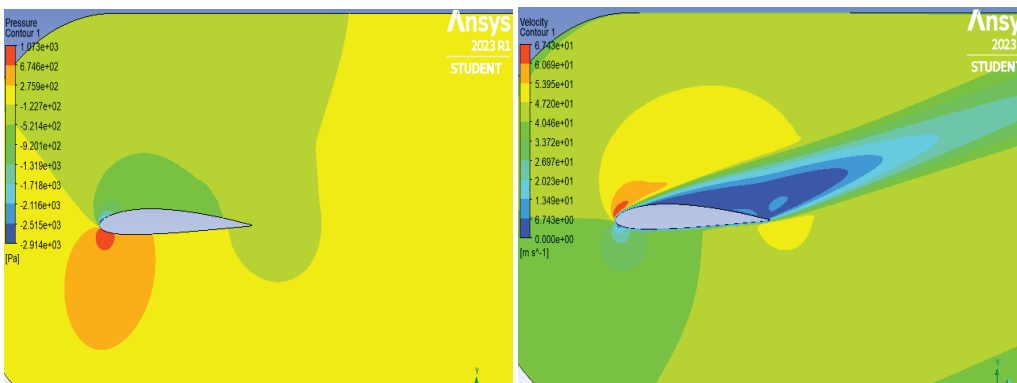
Figure 10. NACA 2412 airfoil pressure and velocity cotour (Angle of attack = 15°).
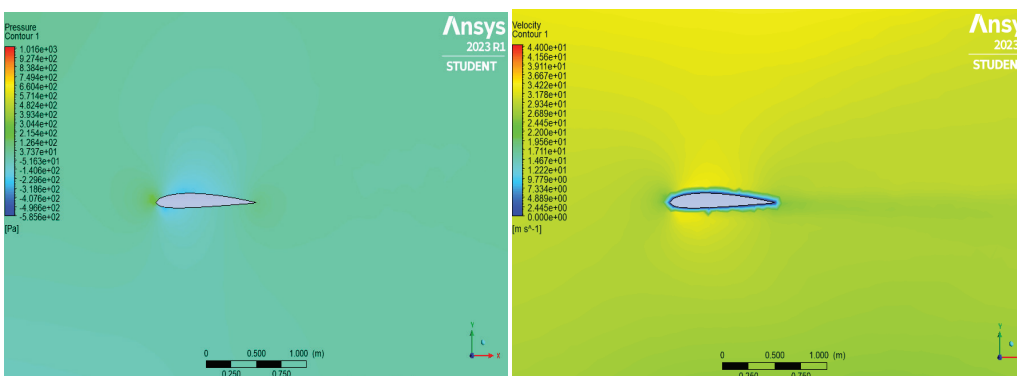
Figure 11. NACA 4412 airfoil pressure and velocity cotour (Angle of attack = 15°).

Table 7. Angle of attack = 15°

AOA = 15°	Lift Force [N]	Drag Force [N]
NACA 2412	19.06	3.32
NACA 4412	59.35	23.60

As depicted in Table 5, there is a noticeable decrease in lift forces and an increase in drag forces for both airfoils. Despite these changes, it is noteworthy that the lift-to-drag ratio remains more favorable in the case of the NACA 2412 airfoil compared to the NACA 4412 airfoil.
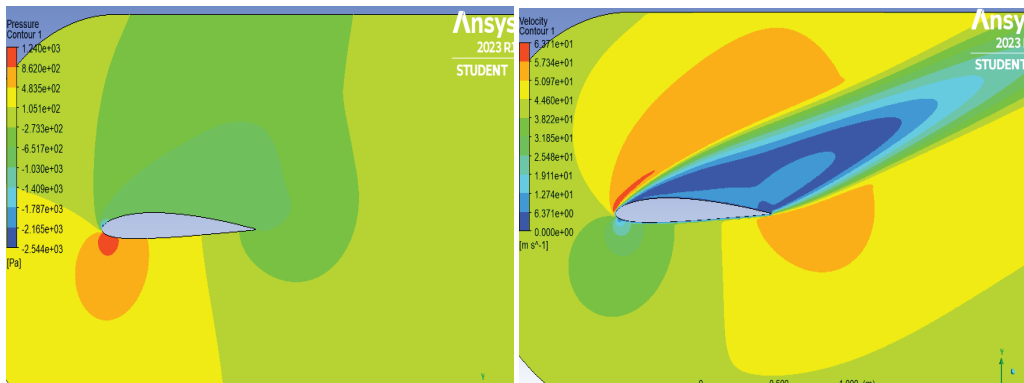
Figure 12. NACA 2412 airfoil pressure and velocity cotour (Angle of attack = 20°).
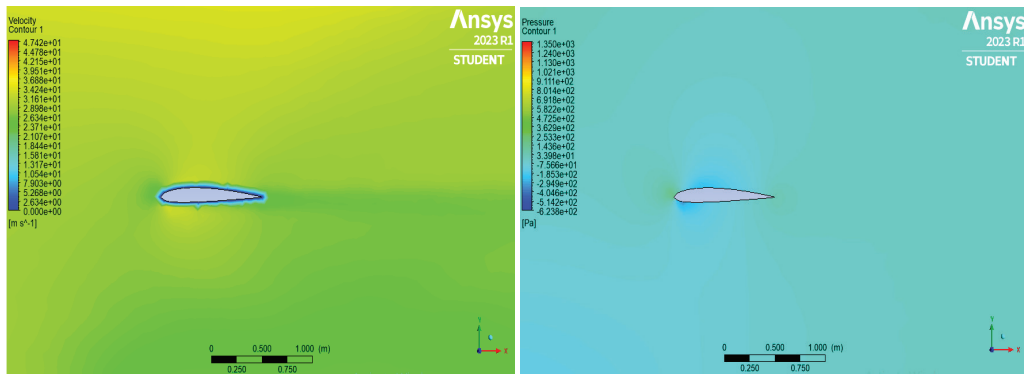
Figure 13. NACA 4412 airfoil pressure and velocity cotour (Angle of attack = 20°).

Table 8. Angle of attack = 20°

AOA = 20°	Lift Force [N]	Drag Force [N]
NACA 2412	12.12	4.25
NACA 4412	19.52	10.85

Table 9. Lift Coefficient

AOA	CL of NACA4412	CL of NACA 2412
0	0.412	0.0589
5	0.912	0.7429
10	1.26	1.1591
15	1.24	0.8412
20	0.908	0.435

This consistent effectiveness in the lift-to-drag ratio for the NACA 2412 airfoil suggests that, even with variations in lift and drag forces, it maintains a superior balance between lift generation and drag resistance. These findings further emphasize the aerodynamic efficiency of the NACA 2412 airfoil compared to the NACA 4412 airfoil under the specified conditions, providing valuable insights for applications where an optimized lift-to-drag ratio is crucial.

Table 7 presents that the decreasing in lift forces and increasing in drag forces in two airfoil, but the lift to drag ratio in NACA 2412 still effective more than NACA 4412 airfoil.

The last case when the angle of attack equals to 20° the stall phenomenon continued and the separation is very clear to show in Figure 12 and Figure 13, the lost in pressure difference is the reason of decreasing in aerodynamics forces.

Table 8 presents the lost in lift force in two airfoils, and that gives us idea about the importence of difference of pressure between the two edges of airfoils, that means that the air flow doesn't generate lift well .

Figure 14 provides a crucial comparison of the lift coefficient (CL) with respect to the angle of attack for the two airfoils under consideration. Significantly, the lift coefficient values of the NACA 4412 airfoil are observed to surpass those of the NACA 2412 airfoil up to a specific angle of attack, as indicated in Table 9. Beyond this point, however, the lift force begins to decrease due to the onset of stall conditions.
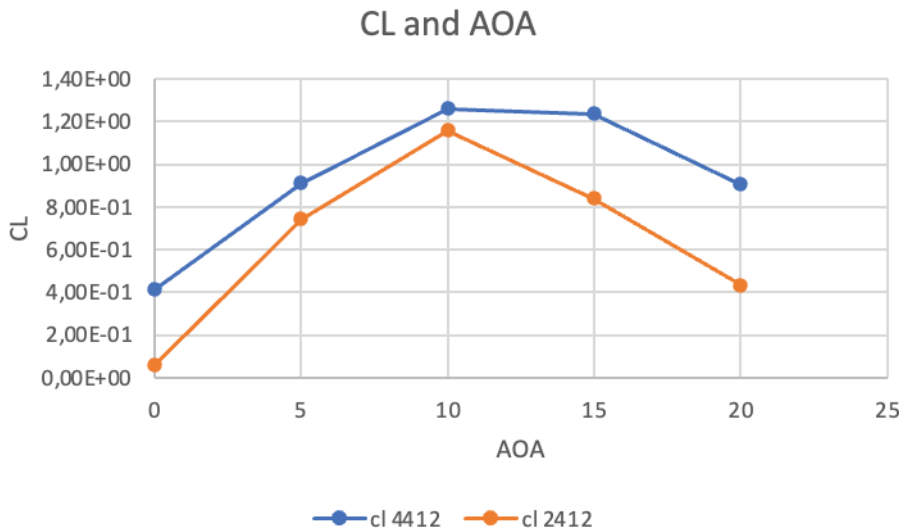
Figure 14. Lift coefficient and angle of attack for NACA 2412 and NACA 4412.

Table 10. Drag Coefficient

AOA	CD of NACA 4412	CD of NACA 2412
0	0.107	0.2316
5	4.21E-02	0.03056
10	6.85E-02	0.05124
15	0.172	0.1522
20	0.2	0.348

certain angle of attack underscores the critical importance of understanding and managing stall conditions for optimal aerodynamic performance.

Lift coefficient one of the most important parameters to give an indicate about the efficiency of airfoils, Figure 14 presents that the comparison between the two airfoils CL with respect to angle of attack, notebly CL values of NACA 4412 larger than NACA 2412 until specific angle of attack in Table 9, then the lift force going down due to stall.

The second parameter had been solced drag coefficient (CD), and from Figure 15 and Table 10. It is seen that the drag force is at its minimum value when the angle of attack is between 5° and 10°, after this angle when air flow starts to getting lost the value of drag force increased. It was determined that the stall effect in NACA 2412 was greater than

This comparison sheds light on the efficiency of the airfoils in terms of lift generation, with the NACA 4412 initially outperforming the NACA 2412 in terms of lift coefficient. The subsequent decline in lift force for both airfoils after a
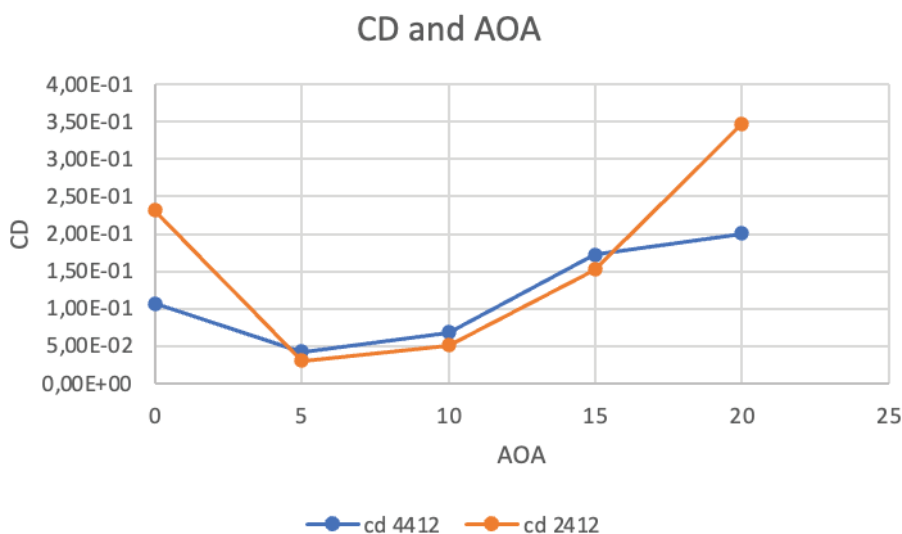
Figure 15. Drag coefficient and angle of attack for NACA 2412 and NACA 4412.
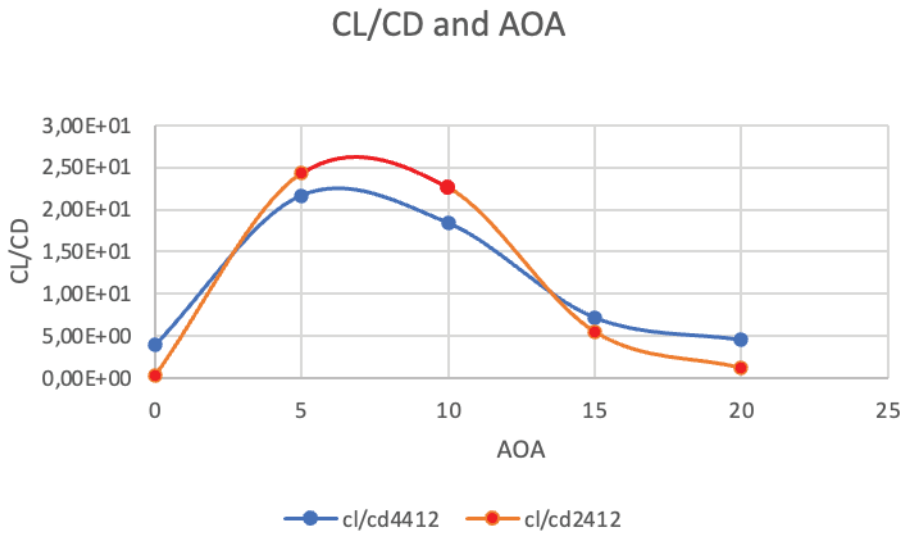
Figure 16. Lift to drag coefficients and angle of attack for NACA 2412 and NACA 4412.
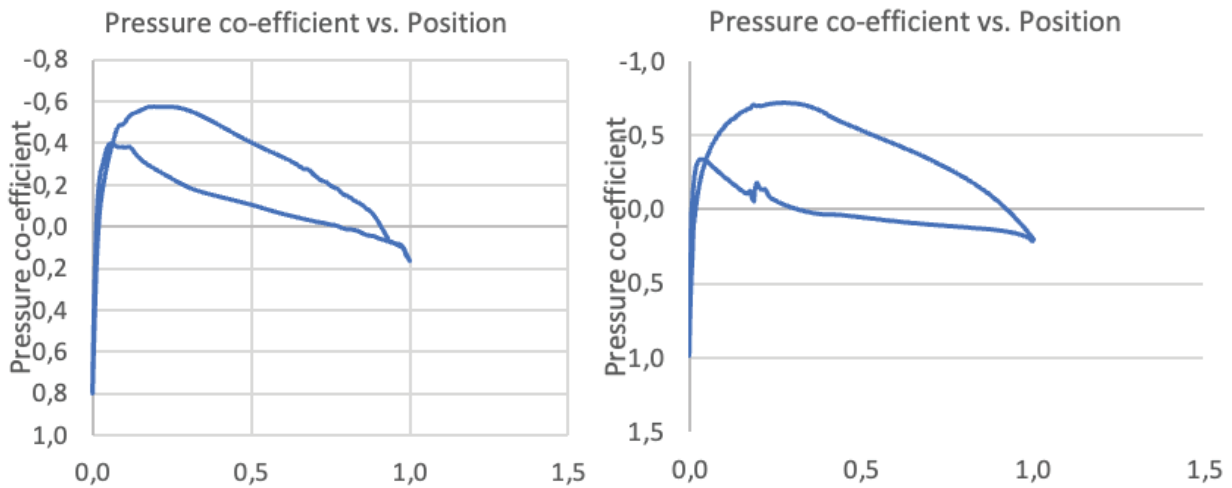
a) At 0° angle of attack
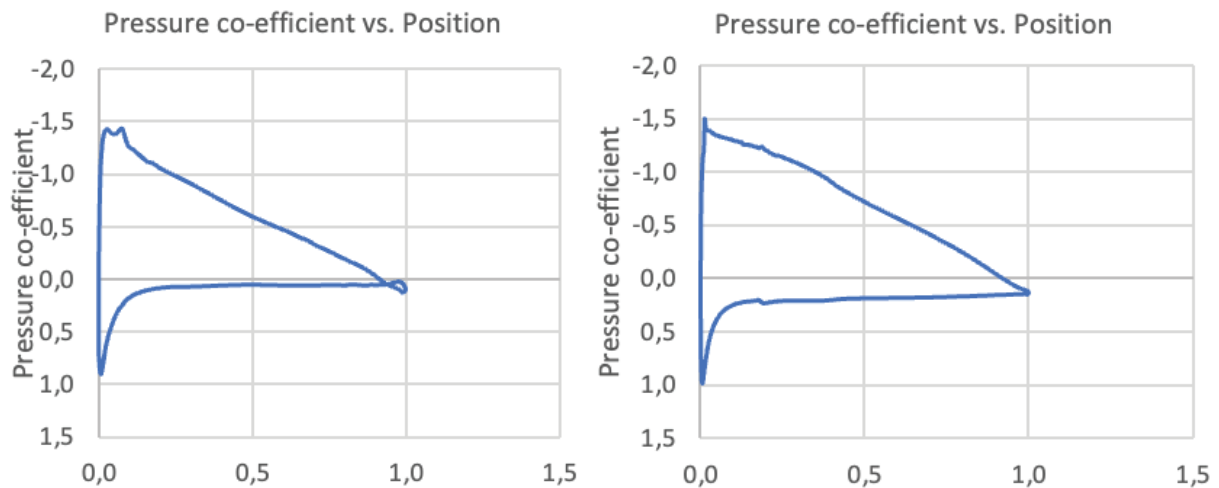
b) At 5° angle of attack
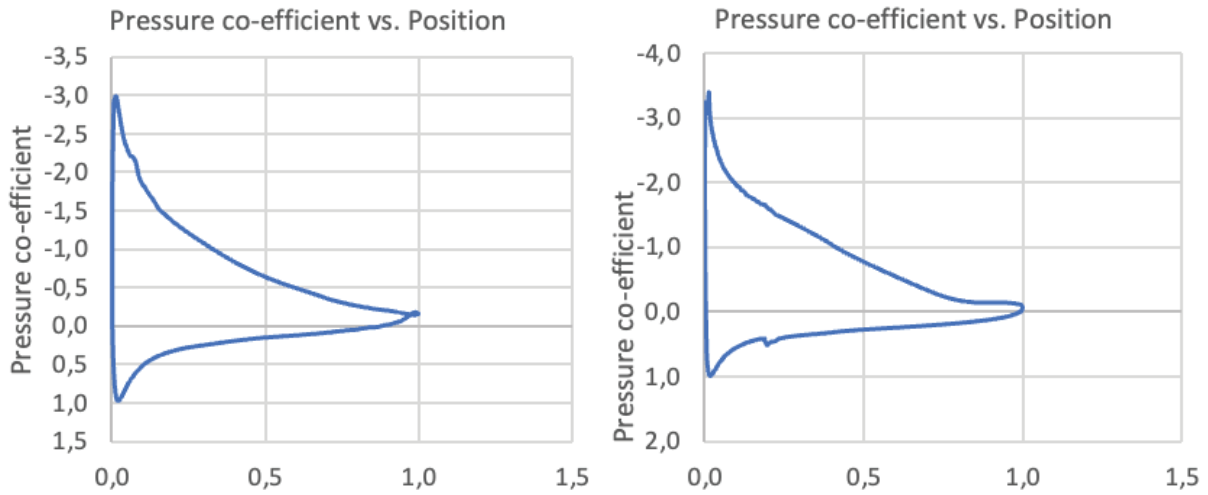
c) At 10° angle of attack
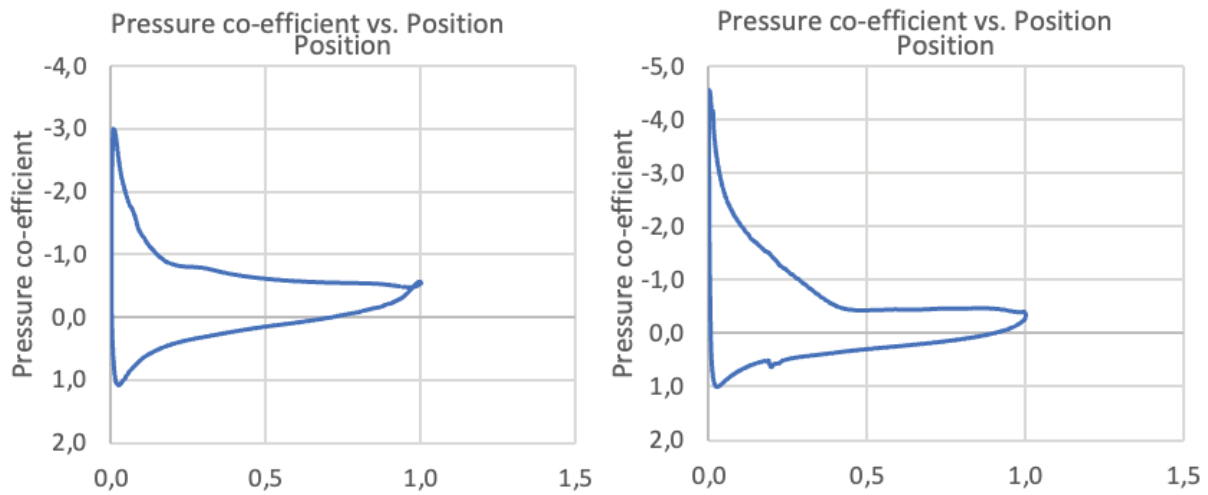
d) At 15° angle of attack
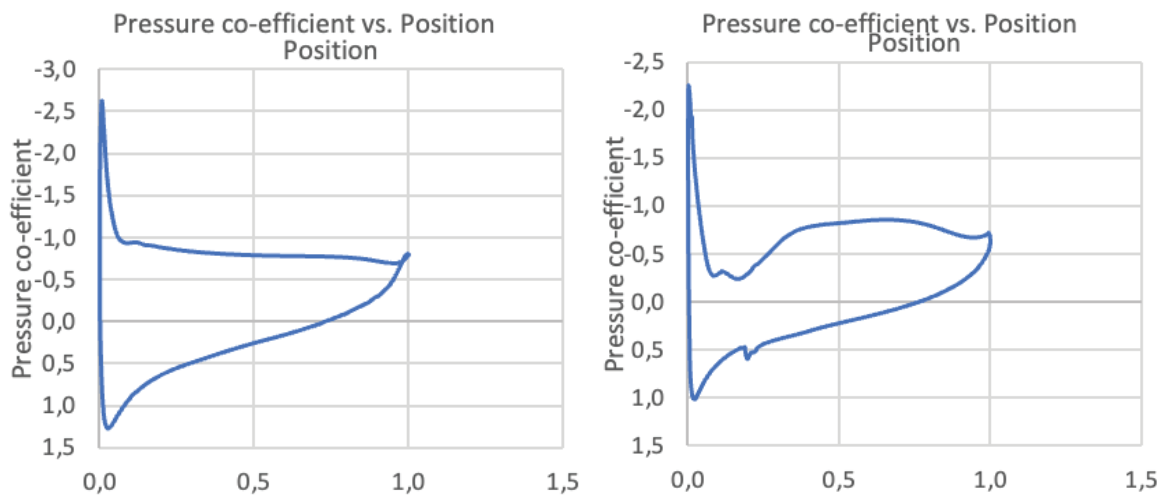
e) At 20° angle of attack

Figure 17. Pressure coefficient vs position for different angle of attack for NACA 2412 and NACA 4412.
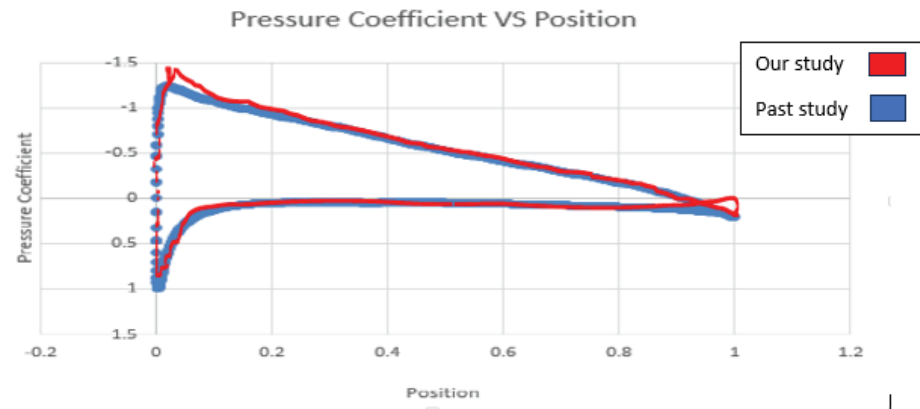
Figure 18. Pressure coefficient comparison when AOA = 5° between our study and past research for NACA 2412 airfoil [5].

in NACA 4412 and the drag coefficient value increased significantly in NACA 2412.

The lift-to-drag ratio C/D is a crucial parameter in aerodynamics that indicates the efficiency of an airfoil. A higher C/D value generally implies a more efficient performance in terms of lift generation relative to drag.

In the context of your statement, it suggests that the NACA 2412 airfoil outperforms the NACA 4412 airfoil in terms of lift-to-drag ratio across various angles of attack. This finding could have practical implications for aircraft or other applications that involve these airfoil profiles. To delve deeper into the interpretation, a higher C/D for NACA 2412 indicates that, for a given amount of drag, the NACA 2412 airfoil is able to produce more lift compared to the NACA 4412. This can be advantageous in terms of achieving better overall aerodynamic efficiency and performance.

The specific angles of attack at which NACA 2412 outperforms NACA 4412, as shown in Figure 16, can provide insights into the airfoils' performance characteristics under different flow conditions. Engineers and researchers often analyze such data to optimize the design of wings and airfoils for specific applications, taking into consideration factors like lift, drag, and their trade-offs.

The pressure coefficient (Cp) is one of most important parameters that describes the flow behaviour around the airfoil, and showing that the pressure distribution at lower and uppre surfaces of airfoil [5].

In Figure 17, the pressure distribution around the airfoil is depicted. Positive values represent pressure on the upper surface, while negative values denote pressure on the lower surface. When the pressure coefficient values in the negative region surpass those in the positive region, it signifies that the airfoil is generating lift force.

In Figure 17a, the angle of attack was set to zero, and it was observed that a significant portion of the pressure values fell within the negative region. However, the disparity in pressure between the two surfaces was relatively minor. As the angle of attack increased the pressure values on

both surfaces gradually rose until reaching a specific angle. Beyond this point, the pressure values began to decrease.

Between angles of attack ranging from 10° to 15° Figure17c and Figure 17d, the pressure difference reaches its maximum value, indicating a substantial increase in lift force generation. It was determined that NACA 2412 has higher values in terms of pressure difference.

Figure 18 serves as a visual validation of the examination conducted, highlighting the close alignment between the results obtained from the two studies. The nearly identical representation in the drawing reaffirms the accuracy and reliability of the analyses performed. Such visual validation is crucial in establishing confidence in the consistency and robustness of the methodologies employed. It not only reinforces the validity of the conducted examination but also underscores the effectiveness of the chosen approach, whether it be experimental or computational. This alignment of results strengthens the credibility of the findings and contributes to a comprehensive understanding of the aerodynamic behaviors under consideration.

CONCLUSION

For five different individual angles of attacks were applied on two airfoils (0°, 5°, 10°.15°, 20°), graphs of velocity and pressure contours while changing angle of attack were plotted and are given in figures, the airfoil has higher lift values when angle of attack equal to 10° than 15° and 20° conditions, when angle of attack equals to 20 lift force getting down, lift force is getting lost due to stall criteria. Lift and drag gives a small change at 5° and 10° angle of attack. From the simulation for two airfoils, it was observed that the flow around NACA 2412 has a smooth behavior with respect to NACA 4412, therefore the efficiency of NACA 2412 is better in aerodynamics approach. Because the lift to drag ratio in NACA 2412 has amount near to 20, but in NACA 4412 the ratio is near to 6. From the definition of NACA the NACA 4412 has a 20% percent larger than

NACA 2412 in mean camber line, and all change in results due to this difference in mean camber of airfoils.

Certainly, the pressure difference is a pivotal parameter in describing airfoil behavior, particularly as it directly contributes to the generation of lift force. In the case under consideration, it is noteworthy that the NACA 2412 airfoil exhibits a larger pressure difference compared to the NACA 4412 airfoil. This disparity in pressure difference is a key factor influencing the observed variations in lift forces between the two airfoils. The larger pressure difference associated with the NACA 2412 airfoil indicates a more effective utilization of aerodynamic principles, contributing to enhanced lift generation. Understanding these pressure differentials is fundamental to comprehending the nuanced aerodynamic characteristics of different airfoil designs, offering valuable insights for optimizing lift performance in practical applications.

The pressure difference is a critical parameter in characterizing the behavior of an airfoil, and it plays a pivotal role in generating lift force. In the case of the NACA 2412 airfoil, there is a notable and larger pressure difference compared to the NACA 4412 airfoil. This observation indicates that, under the specified conditions, the NACA 2412 airfoil is associated with a more significant pressure disparity, contributing to a higher lift force generation. A larger pressure difference is often indicative of a more efficient airfoil design in terms of lift performance. The way pressure varies around an airfoil is crucial for understanding its aerodynamic characteristics, and a favorable pressure distribution can enhance lift while minimizing drag. The specific pressure distribution on the NACA 2412 airfoil, as highlighted by the larger pressure difference, suggests its suitability for applications where increased lift is desirable. This information is valuable for engineers and designers in optimizing airfoil selection based on performance requirements in various contexts.

AUTHORSHIP CONTRIBUTIONS

All authors have contributed to, read, and approved the manuscript in its current form. The conceptualization and manuscript were conducted by DAG and KA. Literature, theory and method was completed by DAG. The Computational Fluid Dynamics analysis was KA.

DATA AVAILABILITY STATEMENT

The authors confirm that the data that supports the findings of this study are available within the article. Raw data that support the finding of this study are available from the corresponding author, upon reasonable request.

CONFLICT OF INTEREST

The author declared no potential conflicts of interest with respect to the research, authorship, and/or publication of this article.

ETHICS

There are no ethical issues with the publication of this manuscript.

REFERENCES

[1] Oukassou K, El Mouhsine S, El Hajjaji A, Kharbouch B. Comparison of the power, lift and drag coefficients of wind turbine blade from aerodynamics characteristics of NACA0012 and NACA2412. Proc Manufact 2019;32:983−990. [CrossRef]

[2] Kulshreshtha A, Gupta SK, Singhal P. FEM/CFD analysis of wings at different angle of attack. Mater Today Proc 2020;26:1638−1643. [CrossRef]

[3] Abood YA, Abdulrazzaq OA, Habib GS, Haseeb ZM. Determination of the Optimum Aerodynamic Parameters in the Design of Wind Turbine Using COMSOL Multiphysics Software. Iraqi J Indust Res 2022;9:77−85. [CrossRef]

[4] Rao YSR, Manohar MS, Praveen SS. CFD simulation of NACA airfoilsat various angles of attack. IOP Conf Ser Mater Sci Engineer 2021;1168:012011. [CrossRef]

[5] Hasan SM, Islam SM, Haque M. Comparison of aerodynamic characteristics of NACA 0012 and NACA 2412 airfoil. IJRASET 2021;9:2037−2045. [CrossRef]

[6] Merryisha S, Rajendran P, Khan SA. CFD Simulation of NACA 2412 airfoil with new cavity shapes. Adv Aircraft Spacecraft Sci 2022;9:131−148.

[7] Nguyen MT, Nguyen NV, Pham MT. Aerodynamic analysis of aircraft wing. VNU J Sci Math Physics 2015;31:68−75.

[8] Shivalingaswamy HB, Panshetty S, Shreyas HS, Sanjay V, Vinayaka N. CFD Analysis of Different Airfoils at Various Angles of Attack. EasyChair No. 10412. Available at: https://easychair.org/publications/preprint/H982/open. Accessed Oct 11, 2024.

[9] Matsson JE, Voth JA, McCain CA, McGraw C. Aerodynamic performance of the NACA 2412 airfoil at Low Reynolds Number. ASEE Annual Conference & Exposition, New Orleans, Louisiana, 2016.

[10] Ganesh Ram RK, Cooper YN, Bhatia V, Karthikeyan R, Periasamy C. Design Optimization and Analysis of NACA 0012 Airfoil using Computational fluid dynamics and Genetic algorithm. Appl Mech Mater 2014;664:111−116. [CrossRef]

[11] Islam MT, Arefin AM, Masud MH, Mourshed M. The effect of Reynolds number on the performance of a modified NACA 2412 airfoil. AIP Conf Proc 2018;1980:040015. [CrossRef]

[12] Noronha NP, Krishna M. Aerodynamic performance comparison of airfoils suggested for small horizontal axis wind turbines. Mater Today Proc 2021;46:2450−2455. [CrossRef]

[13] Singh RK, Ahmed MR, Zullah MA, Lee YH. Design of a low Reynolds number airfoil for small horizontal axis wind turbines. Renew Energy 2012;42:66−76. [CrossRef]

[14] Yakhot V, Orszag SA, Thangam S, Gatski TB, Speziale CG. Development of turbulence models for shear flows by a double expansion technique. Physics Fluids A Fluid Dynamics 1992;4:1510−1520. [CrossRef]

[15] Ravi D, Rajagopal TKR. Numerical investigation on the effect of slit thickness and outlet angle of the bladeless fan for flow optimization using CFD techniques. J Therm Engineer 2023;9:279−296. [CrossRef]

[16] Karasu İ, Açıkel HH, Koca K, Genç MS. Effects of thickness and camber ratio on flow characteristics over airfoils. J Therm Engineer 2020;6:242−252. [CrossRef]

[17] Hussein EQ, Azziz HN, Rashid FL. Aerodynamic study of slotted flap for NACA 24012 airfoil by dynamic mesh techniques and visualization flow. J Therm Engineer 2021;7:230−239. [CrossRef]

[18] Mohammed MA, Husain MA. Numerical simulation of aerodynamic performance of the wing with edge of attack and sinusoidal escape. J Therm Engineer 2024;10:697−709. [CrossRef]

[19] Korkan KD, Camba J III, Morris PM. Aerodynamic data banks for Clark-Y, NACA 4-digit and NACA 16-series airfoil families, 19860021221. Available at: https://ntrs.nasa.gov/api/citations/19860021221/downloads/19860021221.pdf. Accessed Oct 11, 2024.

[20] Soh ZP, Al-Obaidi ASM. Numerical analysis of the shape of dimple on the aerodynamic efficiency of NACA 0012 airfoil. Proceedings of the 6th EURECA 2016 Conference (Paper Number 2ME25), Kuala Lumpur, Malaysia, 2016. pp. 6−7.

[21] Madenci E, Guven I. The Finite Element Method and Applications in Engineering Using ANSYS®. New York: Springer; 2006. pp.15−35.

[22] Kim J, Park YM, Lee J, Kim T, Kim M, Lim J, et al. Numerical investigation of jet angle effect on airfoil stall control. Appl Sci 2019;9:2960. [CrossRef]

[23] Kundu PK, Cohen IM, Dowling DR. Fluid mechanics. Cambridge, MA: Academic Press; 2015.

[24] Feng LH, Choi KS, Wang JJ. Flow control over an airfoil using virtual Gurney flaps. J Fluid Mech 2015;767:595−626. [CrossRef]